
GAS DISCHARGES,
PLASMA

Substantiation of the Two-Temperature Kinetic Model by Comparing Calculations within the Kinetic and Fluid Models of the Positive Column Plasma of a DC Oxygen Discharge

E. A. Bogdanov*, **A. A. Kudryavtsev***, **L. D. Tsendin****, **R. R. Arslanbekov*****,
V. I. Kolobov***, and **V. V. Kudryavtsev******

* *St. Petersburg State University, Universitetskaya nab. 7/9, St. Petersburg, 199034 Russia*
e-mail: akud@ak2138.spb.edu

** *St. Petersburg State Technical University, ul. Politekhnikeskaya 29, St. Petersburg, 195251 Russia*

*** *CFDRC, 215 Wynn Drive, Huntsville, AL, USA*

**** *CFD-Canada, 45 English Ivyway, Toronto*

Received December 23, 2002

Abstract—Results from kinetic and fluid simulations of the positive column plasma of a dc oxygen discharge are compared using commercial CFDRC software (<http://www.cfdrc.com/~cfdplasma>), which enables one to perform numerical simulations in an arbitrary 3D geometry with the use of both the fluid equations for all the components (fluid model) and the kinetic equation for the electron energy distribution function (kinetic model). It is shown that, for both the local and nonlocal regimes of the formation of the electron energy distribution function (EEDF), the non-Maxwellian EEDF can satisfactorily be approximated by two groups of electrons. This allows one to take into account kinetic effects within the conventional fluid model in the simplest way by using the proposed two-temperature approximation of the nonequilibrium and nonlocal EEDF (2T fluid model). © 2003 MAIK “Nauka/Interperiodica”.

The increased interest in discharges in molecular (first of all, electronegative) gases stems from their wide use in modern plasma technologies [1]. The parameters of a gas-discharge plasma can only be determined by employing self-consistent models with allowance for the transport processes and volume plasmochemical reactions involving a great number of atomic and molecular components in different excited and ionization states. To date, the most frequently used model is the hydrodynamic (fluid) model, which has been widely used to describe various plasmochemical facilities (see, e.g., [1–3]). To make an express estimate of the plasma parameters, a simplified version of the model, namely, space-averaged (global) model [4, 5] is also used. In those models, the rate constants K_j of the reactions with the participation of electrons are expressed in Arrhenius form via the ratio of the activation energy to the electron temperature: $K_j \sim \exp(-E_j/T_e)$. In fluid models, the temperature T_e in the exponential dependence $K_j(T_e)$ is deduced from the mean energy $\bar{\varepsilon} = 3T_e/2$ using the energy balance equation for the electron gas.

In order for such a description to be adequate, the electron energy distribution function (EEDF) must be Maxwellian. However, it is well known (see, e.g., [6]) that the electron distribution differs considerably from Maxwellian (with the only exception of the Langmuir paradox in the collisionless (free-fall) regime, when the

EEDF can be well approximated by a Maxwellian distribution [7]). Generally, when the degree of ionization is not too high ($n_e/N < 10^{-3}$), the EEDF is highly non-equilibrium and is depleted of electrons in the energy range corresponding to inelastic collisions ($\varepsilon > \varepsilon_j$). Depending on the relation between the characteristic diffusion length Λ (e.g., $\Lambda = R/2.4$ for a cylinder) and the electron energy relaxation length λ_e , the EEDF is either local (at $\Lambda > \lambda_e$) or nonlocal (at $\Lambda < \lambda_e$) [8]. The procedure of calculating Λ in discharges with different geometrical configurations is described, for example, in [1]. Thus, for plane-parallel geometry ($x = 0, L$), we have $\Lambda = L/\pi$. Let us remember that, in the first approximation, any discharge geometry can be approximately reduced to the plane-parallel geometry by introducing the effective length $L = V/S$, where V is the volume and S is the surface area. The local EEDF is determined by the plasma parameters at a given spatial point and is factorized in the form of the product $f_0(w, r) = n_e(r)f_0^0(w)$, where $n_e(r)$ is the electron density at the point r and w is the kinetic energy. In contrast, the non-local EEDF is determined by the physical parameters (primarily, electric field) in the region with a size on the order of the electron energy relaxation length $\lambda_e \gg \lambda$ (the electron mean free path), rather than those at a given spatial point. In the case of $\lambda_e \gg \Lambda$, the EEDF is a function of the total electron energy $\varepsilon = w + e\phi(r)$ (the

kinetic energy plus the potential energy) and the Boltzmann equation should be averaged over the entire discharge volume [8]. Hence, the characteristics of all the processes with the participation of electrons are determined by this space-averaged EEDF $f_0(\epsilon)$, which can significantly differ from that calculated in the local approximation. Under such conditions, which occur at low pressures ($p\Lambda \leq (0.1-1.0)$ cm torr), attempts to improve the fluid model by refining rate constants obtained with the help of an EEDF calculated in the local approximation are not guaranteed to be free of faults and unacceptable inaccuracy.

Since, for a real nonequilibrium EEDF, the calculations of the rate constants under the assumption of a Maxwellian distribution hardly have any physical sense, it is difficult to even qualitatively estimate the inaccuracy of data thus obtained. An analysis of the transport processes also shows [9] that, for a weakly ionized plasma with a nonlocal EEDF, a closed system of fluid transport equations can only be written for the local regime ($\Lambda > \lambda_e$). In this case, however, the equation of energy for the electron gas does not provide additional information and appears to be redundant. At the same time, in the nonlocal regime with $\Lambda < \lambda_e$, the electron fluid model itself is not physically justified.

In order to self-consistently calculate the parameters of a multicomponent plasma, it is desirable to have a procedure that, on one hand, take into account the nonequilibrium and nonlocal character of the EEDF and, on the other hand, is less time-consuming than the full-scale solution of the Boltzmann equation with allowance for the spatial transport processes. Therefore, it is important to develop a simplified kinetic description based on a physically justified modification of the fluid model for a non-Maxwellian EEDF.

For this purpose, in this paper we compare the kinetic and fluid approaches to the modeling of the plasma of the positive column of a dc oxygen discharge. It is shown that, in accordance with the analysis of [10], the non-Maxwellian distribution function in the fluid model (in both the local and nonlocal regimes of the EEDF formation) can satisfactorily be approximated by two groups of electrons, each of which has its own temperature (mean energy). The temperature T_{et} of the fast electrons determines the rate constants for excitation and ionization. In a steady-state discharge, the ionization frequency (the inverse lifetime) for a given gas species is a function of the only parameter $p\Lambda$ and depends slightly (logarithmically) on it. Hence, at a constant $p\Lambda$ value, the temperature T_{et} is almost the same for different types of gas discharges [10]. The temperature T_{eb} of the low-energy part of the EEDF determines the plasma ambipolar fields. In some important cases (see below), this temperature depends only on the gas species. To adapt the classical fluid model in order to determine the parameters of a gas-discharge plasma, we propose a 2T fluid model in which the rate constants of the processes with the participation of

electrons are found with the help of a proper EEDF approximation (see Eqs. (1), (2)).

We chose the positive column of a dc discharge because it is a very suitable test object and has been intensely studied for both atomic and molecular gases. In turn, among the electronegative gases, most of the studies and calculations within different approximations have been made for oxygen (see, e.g., [11–15]).

To calculate the discharge parameters, we used commercial software developed by the CFD Research Corporation, Huntsville, AL, USA [16, 17]. The self-consistent model of a discharge plasma, the numerical iteration scheme, and the technique for solving the set of equations are described in detail in [16, 17]. In simulations, the main model parameters are the discharge geometry, the pressure and composition of the gas, and the specific power W deposited in the discharge. A specific feature of the dc discharge is that we can specify the current density j instead of W using the simple relation $W = jE$. The self-consistent electric field was found from Poisson's equation. Heavy particles were described in the fluid model. The parameters of the electron gas could be found both by using the fluid equations for the balance of the electron density and energy and by solving the kinetic equation for the EEDF. Since this study is aimed at comparing the fluid and kinetic descriptions of the electron component, all other factors being the same, some problems that are not directly related to the electron kinetics were not analyzed in detail. In particular, we did not take into account the heating of the heavy components [12, 15], because the physical consequence of this effect is of minor importance when calculating the EEDF. This issue will be considered in a separate paper. Here, the gas and ion temperatures were assumed to be constant over the discharge cross section and equal to room temperature.

The accounted volume plasmachemical processes with the participation of various atomic and molecular oxygen states are listed in Table 1. In the fluid model, the rate constants of the processes with the participation of electrons were obtained by convoluting the corresponding cross sections with a Maxwellian EEDF, whereas in the kinetic model, they were obtained by convoluting these cross sections with an EEDF calculated with the help of the CDFRC Kinetic Module [16, 17].

For definiteness, we considered conditions corresponding to the positive column of a dc discharge in a 12-mm-diameter glass tube at gas pressures of 0.05–3 torr and discharge currents of 5–200 mA. These conditions correspond to those investigated in [12, 18], in which, in our opinion, the most detailed experimental and theoretical studies of the positive column of a dc oxygen discharge were performed.

Typical EEDFs obtained by self-consistently simulating the dc discharge plasma at gas pressures of $p = 1$ and 0.15 torr are shown in Figs. 1 and 2. It can be seen

Table 1. Volume plasmachemical processes involved in simulations

No.	Reaction	$\Delta\epsilon$, eV	Rate constant
Elastic electron scattering			
1	$e + O_2 \longrightarrow e + O_2$	0	Cross section (CS) [1]
2	$e + O_2(a^1\Delta) \longrightarrow e + O_2(a^1\Delta)$	0	CS (copy of 1)
3	$e + O_2(b^1\Sigma) \longrightarrow e + O_2(b^1\Sigma)$	0	CS (copy of 1)
4	$e + O_2(v_1) \longrightarrow e + O_2(v_1)$	0	CS (copy of 1)
5	$e + O_2(Ry) \longrightarrow e + O_2(Ry)$	0	CS (copy of 1)
6	$e + O \longrightarrow e + O$	0	CS [3]
7	$e + O(^1D) \longrightarrow e + O(^1D)$	0	CS (copy of 6)
8	$e + O(^1S) \longrightarrow e + O(^1S)$	0	CS (copy of 6)
9	$e + O_3 \longrightarrow e + O_3$	0	CS [5]
Inelastic processes with the participation of electrons			
10	$e + O_2 \longrightarrow O_- + O$	3.637	CS [1]
11	$e + O_2 \longrightarrow e + O_2(v_1)$	0.19	CS [1]
12	$e + O_2(v_1) \longrightarrow e + O_2$	-0.19	CS [1]
13	$e + O_2 \longrightarrow e + O_2(v_2)$	0.38	CS [1]
14	$e + O_2 \longrightarrow e + O_2(v_3)$	0.57	CS [1]
15	$e + O_2 \longrightarrow e + O_2(v_4)$	0.75	CS [1]
16	$e + O_2 \longrightarrow e + O_2(a^1\Delta)$	0.97	CS [1]
17	$e + O_2(a^1\Delta) \longrightarrow e + O_2$	-0.97	Obtained from a detailed balance with c 16
18	$e + O_2 \longrightarrow e + O_2(b^1\Sigma)$	1.63	CS [1]
19	$e + O_2(b^1\Sigma) \longrightarrow e + O_2$	-1.63	Obtained from a detailed balance with c 18
20	$e + O_2 \longrightarrow e + 2O$	5.12	CS [1]
21	$e + O_2 \longrightarrow e + O + O(^1D)$	7.1	CS [1]
22	$e + O_2 \longrightarrow 2e + O_{2+}$	12.6	CS [1]
23	$e + O_2 \longrightarrow 2e + O + O_+$	18.8	CS [1]
24	$e + 2O_2 \longrightarrow O_2 + O_{2-}$	-5.03	$k_{24} = 3.6E - 43T_e^{-0.5} \text{ m}^6/\text{s}$
25	$e + O_{2+} \longrightarrow 2O$	-6.96	Cross section (CS) from 2
26	$e + O_{2+} \longrightarrow O + O(^1D)$	-5.0	CS [2]
27	$e + O_2(a^1\Delta) \longrightarrow 2e + O_{2+}$	-11.63	CS [3]
28	$e + O_2(b^1\Sigma) \longrightarrow 2e + O_{2+}$	-10.97	$k_{28} = 1.3E - 15T_e^{-1.1} \exp(-10.43/T_e) \text{ m}^3/\text{s}$
29	$e + O_3 \longrightarrow O_- + O_2$	-0.42	CS [5]
30	$e + O_3 \longrightarrow O + O_{2-}$	0.60	CS [5]
31	$e + O \longrightarrow e + O(^1D)$	1.97	CS [4]
32	$e + O \longrightarrow e + O(^1S)$	4.24	CS [4]
33	$e + O(^1S) \longrightarrow e + O$	-4.24	Obtained from a detailed balance with c 32
34	$e + O \longrightarrow 2e + O_+$	13.67	CS [4]
35	$e + O(^1D) \longrightarrow e + O$	-1.97	CS [4]
36	$e + O(^1D) \longrightarrow 2e + O_+$	11.7	CS [4]
37	$e + O(^1S) \longrightarrow 2e + O_+$	9.43	$k_{37} = 6.6E - 15T_e^{0.6} \exp(-9.43/T_e) \text{ m}^3/\text{s}$
38	$e + O_- \longrightarrow 2e + O$	1.53	$k_{38} = 1.95E - 18T_e^{0.5} \exp(-3.4/T_e) \text{ m}^3/\text{s}$
39	$e + O_+ \longrightarrow O(^1D)$	-11.7	$k_{39} = 5.3E - 19T_e^{-0.5} \text{ m}^3/\text{s}$
40	$2e + O_+ \longrightarrow e + O(^1D)$	-11.7	$k_{40} = 5.12E - 36T_e^{-4.5} \text{ m}^6/\text{s}$
41	$e + O \longrightarrow e + O(3s^5S_0)$	9.15	CS [4]
42	$e + O \longrightarrow e + O(3s^3S_0)$	9.51	CS [4]
43	$e + O \longrightarrow e + O(3p^5P)$	10.73	CS [4]
44	$e + O \longrightarrow e + O(3p^3P)$	10.98	CS [4]
45	$e + O_2 \longrightarrow e + O_2(Rot)$	0.02	CS [1]
46	$e + O_2 \longrightarrow e + O_2(v_5)$	0.19	CS [1]
47	$e + O_2 \longrightarrow e + O_2(v_6)$	0.38	CS [1]
48	$e + O_2 \longrightarrow e + O_2(^1\Pi_g)$	8.4	CS [1]

Table 1. (Contd.)

No.	Reaction	$\Delta\varepsilon$, eV	Rate constant
49	$e + O_2 \longrightarrow e + O_2(a^1\Sigma_u^+)$	10.0	CS [1]
50	$e + O_2 \longrightarrow e + O_2 + h\nu$ (130 nm)	9.547	CS [1]
51	$e + O_2(a^1\Delta) \longrightarrow e + O_2(b^1\Sigma)$	0.65	CS [1]
52	$e + O_2(b^1\Sigma) \longrightarrow e + O_2(a^1\Delta)$	-0.65	CS [2]
53	$e + O_2 \longrightarrow e + O_2(Ry)$	4.47	CS [1]
54	$e + O_2(Ry) \longrightarrow e + O_2$	-4.47	CS [2]
55	$e + O_2(a^1\Delta) \longrightarrow e + O_2(Ry)$	3.45	CS [2]
56	$e + O_2 \longrightarrow e + O + O(^1S)$	9.36	CS [2]
57	$e + O_2(a^1\Delta) \longrightarrow O + O_-$	2.57	CS [2]
58	$e + O_{2+} \longrightarrow O_2(Ry)$	-7.66	CS [2]
59	$e + O_2 + O_3 \longrightarrow O_2 + O_{3-}$	-0.679	$4.6E - 40 \text{ m}^3/\text{s}$
60	$e + O_{2+} \longrightarrow O + O(^1S)$	-2.73	$2.42E - 13 T_e^{-0.55} \text{ m}^3/\text{s}$
61	$e + O_{4+} \longrightarrow 2O_2$	-0.8	$2.42E - 11 T_e^{-0.5} \text{ m}^3/\text{s}$
62	$e + O_{4+} \longrightarrow O_2 + O_2(Ry)$	3.68	$2.425E - 12 T_e^{-0.5} \text{ m}^3/\text{s}$
Reactions involving heavy particles			
63	$O_- + O_{2+} \longrightarrow O + O_2$		$k_{63} = 5.96E - 11 T_g^{-1} \text{ m}^3/\text{s}$
64	$O_- + O_{2+} \longrightarrow 3O$		$k_{64} = 1E - 13 \text{ m}^3/\text{s}$
65	$O_- + O_+ \longrightarrow 2O$		$k_{65} = 5.96E - 11 T_g^{-1} \text{ m}^3/\text{s}$
66	$O_{2-} + O_{2+} \longrightarrow 2O_2$		$k_{66} = 5.96E - 11 T_g^{-1} \text{ m}^3/\text{s}$
67	$O_{2-} + O_{2+} \longrightarrow O_2 + 2O$		$k_{67} = 1E - 13 \text{ m}^3/\text{s}$
68	$O_+ + O_{2-} \longrightarrow O_2 + O$		$k_{68} = 5.96E - 11 T_g^{-1} \text{ m}^3/\text{s}$
69	$O_{2+} + O_{3-} \longrightarrow O_2 + O_3$		$k_{69} = 5.96E - 11 T_g^{-1} \text{ m}^3/\text{s}$
70	$O_{2+} + O_{3-} \longrightarrow 2O + O_3$		$k_{70} = 1E - 13 \text{ m}^3/\text{s}$
71	$O_+ + O_{3-} \longrightarrow O + O_3$		$k_{71} = 5.96E - 11 T_g^{-1} \text{ m}^3/\text{s}$
72	$O_- + O_{2+} + O_2 \longrightarrow O + 2O_2$		$k_{72} = 3.066E - 31 T_g^{-2.5} \text{ m}^6/\text{s}$
73	$O_- + O_+ + O_2 \longrightarrow 2O + O_2$		$k_{73} = 3.066E - 31 T_g^{-2.5} \text{ m}^3/\text{s}$
74	$O + O_- \longrightarrow O_2 + e$		$k_{74} = 1.159E - 17 T_g^{0.5} \text{ m}^3/\text{s}$
75	$O_- + O_2(a^1\Delta) \longrightarrow O_3 + e$		$k_{75} = 1.738E - 17 T_g^{0.5} \text{ m}^3/\text{s}$
76	$O_- + O_2(b^1\Sigma) \longrightarrow O_2 + O + e$		$k_{76} = 4E - 17 T_g^{0.5} \text{ m}^3/\text{s}$
77	$O_- + O_2 \longrightarrow O_3 + e$		$k_{77} = 2.896E - 22 T_g^{0.5} \text{ m}^3/\text{s}$
78	$O_- + O_3 \longrightarrow 2O_2 + e$		$k_{78} = 1.744E - 17 T_g^{0.5} \text{ m}^3/\text{s}$
79	$O_- + O_3 \longrightarrow O + O_{3-}$		$k_{79} = 1.153E - 17 T_g^{0.5} \text{ m}^3/\text{s}$
80	$O_- + O_3 \longrightarrow O_2 + O_{2-}$		$k_{80} = 5.909E - 19 T_g^{0.5} \text{ m}^3/\text{s}$
81	$O + O_{2-} \longrightarrow O + O_{2-}$		$k_{81} = 8.69E - 18 T_g^{0.5} \text{ m}^3/\text{s}$
82	$O + O_{2-} \longrightarrow O_3 + e$		$k_{82} = 8.69E - 18 T_g^{0.5} \text{ m}^3/\text{s}$
83	$O_2(a^1\Delta) + O_{2-} \longrightarrow 2O_2 + e$		$k_{83} = 1.159E - 17 T_g^{0.5} \text{ m}^3/\text{s}$
84	$O_{2-} + O_3 \longrightarrow O_2 + O_{3-}$		$k_{84} = 3.746E - 17 T_g^{0.5} \text{ m}^3/\text{s}$
85	$O + O_{3-} \longrightarrow O_2 + O_{2-}$		$k_{85} = 1.448E - 17 T_g^{0.5} \text{ m}^3/\text{s}$
86	$O + O_+ + O_2 \longrightarrow O_2 + O_{2+}$		$k_{86} = 5.793E - 43 T_g^{0.5} \text{ m}^6/\text{s}$

Table 1. (Contd.)

No.	Reaction	$\Delta\epsilon$, eV	Rate constant
87	$O_+ + O_2 \longrightarrow O + O_{2+}$		$k_{87} = 1.953E - 16T_g^{-0.4} \text{ m}^3/\text{s}$
88	$O_+ + O_3 \longrightarrow O_2 + O_{2+}$		$k_{88} = 1E - 16 \text{ m}^3/\text{s}$
89	$O(^1D) + O \longrightarrow 2O$		$k_{89} = 8E - 18 \text{ m}^3/\text{s}$
90	$O(^1D) + O_2 \longrightarrow O + O_2(b^1\Sigma)$		$k_{90} = 2.56E - 17\exp(+67/T_g) \text{ m}^3/\text{s}$
91	$O(^1D) + O_2 \longrightarrow O + O_2(a^1\Delta)$		$k_{91} = 1.6E - 18\exp(+67/T_g) \text{ m}^3/\text{s}$
92	$O(^1D) + O_2 \longrightarrow O + O_2$		$k_{92} = 4.8E - 18\exp(+67/T_g) \text{ m}^3/\text{s}$
93	$O(^1D) + O_3 \longrightarrow 2O + O_2$		$k_{93} = 1.2E - 16 \text{ m}^3/\text{s}$
94	$O(^1D) + O_3 \longrightarrow 2O_2$		$k_{94} = 1.2E - 16 \text{ m}^3/\text{s}$
95	$O(^1S) + O_2 \longrightarrow O(^1D) + O_2$		$k_{95} = 3.2E - 16\exp(-850/T_g) \text{ m}^3/\text{s}$
96	$O(^1S) + O_2 \longrightarrow O + O_2$		$k_{96} = 1.6E - 18\exp(-850/T_g) \text{ m}^3/\text{s}$
97	$O(^1S) + O_2(a^1\Delta) \longrightarrow O + O_2$		$k_{97} = 1.1E - 16 \text{ m}^3/\text{s}$
98	$O(^1S) + O_2(a^1\Delta) \longrightarrow O(^1D) + O_2(b^1\Sigma)$		$k_{98} = 2.9E - 17 \text{ m}^3/\text{s}$
99	$O(^1S) + O_2(a^1\Delta) \longrightarrow 3O$		$k_{99} = 3.2E - 17 \text{ m}^3/\text{s}$
100	$O(^1S) + O \longrightarrow O(^1D) + O$		$k_{100} = 1.67E - 17\exp(-300/T_g) \text{ m}^3/\text{s}$
101	$O(^1S) + O \longrightarrow 2O$		$k_{101} = 3.33E - 17\exp(-300/T_g) \text{ m}^3/\text{s}$
102	$O(^1S) + O_3 \longrightarrow 2O_2$		$k_{102} = 5.8E - 16 \text{ m}^3/\text{s}$
103	$O_2(a^1\Delta) + O \longrightarrow O_2 + O$		$k_{103} = 2E - 22 \text{ m}^3/\text{s}$
104	$O_2(a^1\Delta) + O_2 \longrightarrow 2O_2$		$k_{104} = 3E - 24\exp(-200/T_g) \text{ m}^3/\text{s}$
105	$2O_2(a^1\Delta) \longrightarrow 2O_2$		$k_{105} = 9E - 23\exp(-560/T_g) \text{ m}^3/\text{s}$
106	$2O_2(a^1\Delta) \longrightarrow O_2 + O_2(b^1\Sigma)$		$k_{106} = 9E - 23\exp(-560/T_g) \text{ m}^3/\text{s}$
107	$2O_2(a^1\Delta) + O_2 \longrightarrow 2O_3$		$k_{107} = 1E - 43\exp(-560/T_g) \text{ m}^3/\text{s}$
108	$2O_2(a^1\Delta) + O_2 \longrightarrow 2O_3$		$k_{108} = 1.709E - 28T_g \text{ m}^3/\text{s}$
109	$O_2(a^1\Delta) + O_3 \longrightarrow 2O_2 + O$		$k_{109} = 5.2E - 17\exp(-2840/T_g) \text{ m}^2/\text{s}$
110	$2O_2(b^1\Sigma) \longrightarrow O_2(a^1\Delta) + O_2$		$k_{110} = 2.085E - 24T_g^{0.5} \text{ m}^3/\text{s}$
111	$O_2(b^1\Sigma) + O_2 \longrightarrow O_2(a^1\Delta) + O_2$		$k_{111} = 2.085E - 25T_g^{0.5} \text{ m}^3/\text{s}$
112	$O_2(b^1\Sigma) + O_2 \longrightarrow 2O_2$		$k_{112} = 2.317E - 28T_g^{0.5} \text{ m}^3/\text{s}$
113	$O_2(b^1\Sigma) + O \longrightarrow O_2(a^1\Delta) + O$		$k_{113} = 4.171E - 21T_g^{0.5} \text{ m}^3/\text{s}$
114	$O_2(b^1\Sigma) + O \longrightarrow O_2 + O$		$k_{114} = 4.634E - 22T_g^{0.5} \text{ m}^3/\text{s}$
115	$O_2(b^1\Sigma) + O_3 \longrightarrow 2O_2 + O$		$k_{115} = 4.246E - 19T_g^{0.5} \text{ m}^3/\text{s}$
116	$O_2(b^1\Sigma) + O_3 \longrightarrow O_2(a^1\Delta) + O_3$		$k_{116} = 4.246E - 19T_g^{0.5} \text{ m}^3/\text{s}$
117	$O_2(b^1\Sigma) + O_3 \longrightarrow O_2 + O_3$		$k_{117} = 4.246E - 19T_g^{0.5} \text{ m}^3/\text{s}$
118	$O_2(v_1) + O \longrightarrow O_2 + O$		$k_{118} = 5.793E - 22T_g^{0.5} \text{ m}^3/\text{s}$
119	$O_2(v_1) + O_2 \longrightarrow 2O_2$		$k_{119} = 5.793E - 22T_g^{0.5} \text{ m}^3/\text{s}$
120	$2O + O_2 \longrightarrow 2O_2$		$k_{120} = 9.268E - 45T_g^{-0.63} \text{ m}^6/\text{s}$
121	$3O \longrightarrow O + O_2$		$k_{121} = 3.334E - 44T_g^{-0.63} \text{ m}^6/\text{s}$
122	$2O + O_2 \longrightarrow O_2(a^1\Delta) + O_2$		$k_{122} = 6.987E - 46T_g^{-0.63} \text{ m}^6/\text{s}$
123	$3O \longrightarrow O_2(a^1\Delta) + O$		$k_{123} = 2.509E - 45T_g^{-0.63} \text{ m}^6/\text{s}$
124	$O + 2O_2 \longrightarrow O_3 + O_2$		$k_{124} = 5.081E - 39T_g^{-2.8} \text{ m}^6/\text{s}$
125	$2O + O_2 \longrightarrow O + O_3$		$k_{125} = 3.166E - 43T_g^{-1.2} \text{ m}^6/\text{s}$
126	$O + O_3 \longrightarrow 2O_2$		$k_{126} = 8E - 18\exp(-2060/T_g) \text{ m}^3/\text{s}$
127	$O_2 + O_3 \longrightarrow O + 2O_2$		$k_{127} = 1.56E - 15\exp(-11490/T_g) \text{ m}^3/\text{s}$

Table 1. (Contd.)

No.	Reaction	$\Delta\epsilon$, eV	Rate constant
128	$O_2(Ry) \longrightarrow O_2$	$k_{128} = 0.015 \text{ s}^{-1}$	
129	$O_2 + O_2(Ry) \longrightarrow O_2 + O_2(a^1\Delta)$	$k_{129} = 1.86E - 19 \text{ m}^3/\text{s}$	
130	$O_2 + O_2(Ry) \longrightarrow O_2 + O_2(b^1\Sigma)$	$k_{130} = 1.86E - 19 \text{ m}^3/\text{s}$	
131	$O(^1D) + O_2(a^1\Delta) \longrightarrow O_2 + O$	$k_{131} = 1E - 17 \text{ m}^3/\text{s}$	
132	$O(^1S) + O_2 \longrightarrow O + O_2(a^1\Delta)$	$k_{132} = 1.5E - 18 \exp(-850/T_g) \text{ m}^3/\text{s}$	
133	$O(^1S) + O_2 \longrightarrow O + O_2(b^1\Sigma)$	$k_{133} = 7.3E - 19 \exp(-850/T_g) \text{ m}^3/\text{s}$	
134	$O(^1S) + O_2 \longrightarrow O + O_2(Ry)$	$k_{134} = 7.3E - 19 \exp(-850/T_g) \text{ m}^3/\text{s}$	
135	$O(^1S) + O_2(a^1\Delta) \longrightarrow O + O_2(Ry)$	$k_{135} = 1.3E - 16 \text{ m}^3/\text{s}$	
136	$O_2(b^1\Sigma) + O_3 \longrightarrow O_2(a^1\Delta) + O_3$	$k_{136} = 7.1E - 18 \text{ m}^3/\text{s}$	
137	$O + O_2 + O_2(a^1\Delta) \longrightarrow O_2(b^1\Sigma) + O_3$	$k_{137} = 1.56E - 40 T_g^{-1.5} \text{ m}^6/\text{s}$	
138	$O + O_2 + O_2(a^1\Delta) \longrightarrow O + 2O_2$	$k_{138} = 3E - 44 \text{ m}^6/\text{s}$	
139	$O + O_3 \longrightarrow O_2 + O_2(a^1\Delta)$	$k_{139} = 2.4E - 19 \exp(-2060/T_g) \text{ m}^3/\text{s}$	
140	$O + O_3 \longrightarrow O_2 + O_2(b^1\Sigma)$	$k_{140} = 8E - 20 \exp(-2060/T_g) \text{ m}^3/\text{s}$	
141	$2O_3 \longrightarrow O + O_2 + O_3$	$k_{141} = 1.65E - 15 \exp(-11435/T_g) \text{ m}^3/\text{s}$	
142	$2O + O_2 \longrightarrow O_2 + O_2(Ry)$	$k_{142} = 1.2E - 46 \text{ m}^6/\text{s}$	
143	$2O + O_2 \longrightarrow O_2 + O_2(b^1\Sigma)$	$k_{143} = 7.6E - 44 T_g^{-1} \exp(-170/T_g) \text{ m}^6/\text{s}$	
144	$O + O_2 + O_3 \longrightarrow 2O_3$	$k_{144} = 1.3E - 41 T_g^{-2} \text{ m}^6/\text{s}$	
145	$2O_2 + O_{2+} \longrightarrow O_2 + O_{4+}$	$k_{145} = 1.25E - 38 T_g^{-1.5} \text{ m}^6/\text{s}$	
146	$O_2(a^1\Delta) + O_{4+} \longrightarrow 2O_2 + O_{2+}$	$k_{146} = 1E - 16 \text{ m}^3/\text{s}$	
147	$O_2(b^1\Sigma) + O_{4+} \longrightarrow 2O_2 + O_{2+}$	$k_{147} = 1E - 16 \text{ m}^3/\text{s}$	
148	$O + O_{4+} \longrightarrow O_{2+} + O_3$	$k_{148} = 3E - 16 \text{ m}^3/\text{s}$	
149	$O_2 + O_{4+} \longrightarrow 2O_2 + O_{2+}$	$k_{149} = 0.02673 T_g^{-4} \exp(-5030/T_g) \text{ m}^3/\text{s}$	
150	$O_- + O_2(a^1\Delta) \longrightarrow O + O_{2-}$	$k_{150} = 3.3E - 17 \text{ m}^3/\text{s}$	
151	$O_- + O_2 \longrightarrow O + O_{2-}$	$k_{151} = 1E - 20 \text{ m}^3/\text{s}$	
152	$O_- + O_2(a^1\Delta) \longrightarrow O + O_2 + e$	$k_{152} = 2E - 16 \exp(-15000/T_g) \text{ m}^3/\text{s}$	
153	$O_- + 2O_2 \longrightarrow O_2 + O_{3-}$	$k_{153} = 3.3E - 40 T_g^{-1} \text{ m}^6/\text{s}$	
154	$O_{2-} + O_2 \longrightarrow 2O_2 + e$	$k_{154} = 2E - 16 \exp(-5338/T_g) \text{ m}^3/\text{s}$	
155	$O_- + O_+ \longrightarrow O_2$	$k_{155} = 2.7E - 13 \text{ m}^3/\text{s}$	
156	$O_- + O_{4+} \longrightarrow O_2 + O_3$	$k_{156} = 6.9E - 12 T_g^{-0.5} \text{ m}^3/\text{s}$	
157	$O_- + O_2 + O_{2+} \longrightarrow O_2 + O_3$	$k_{157} = 2E - 37 \text{ m}^6/\text{s}$	
158	$O_{2-} + O_{2+} + O_2 \longrightarrow 3O_2$	$k_{158} = 2E - 37 \text{ m}^6/\text{s}$	
159	$O_{2-} + O_{4+} \longrightarrow 3O_2$	$k_{159} = 1E - 13 \text{ m}^3/\text{s}$	
160	$O + O_{3-} \longrightarrow 2O_2 + e$	$k_{160} = 3E - 16 \text{ m}^3/\text{s}$	
161	$O_2 + O_{3-} \longrightarrow 2O_2 + O_-$	$k_{161} = 1.62E - 6 T_g^{-2} \exp(-18260/T_g) \text{ m}^3/\text{s}$	
162	$O_{3-} + O_{4+} \longrightarrow 3O_2 + O$	$k_{162} = 1E - 13 \text{ m}^3/\text{s}$	
163	$O_2 + O_{2-} + O_{4+} \longrightarrow 4O_2$	$k_{163} = 4E - 38 \text{ m}^6/\text{s}$	
164	$O_2 + O_{3-} + O_{4+} \longrightarrow 4O_2 + O$	$k_{164} = 4E - 38 \text{ m}^6/\text{s}$	

Note: T_e is the electron temperature in eV; T_g is the gas temperature in K; O and O_2 are the $O(^3P)$ and $O_2(X^3\Sigma_g^-)$ ground states of an oxygen atom and molecule, respectively; $O_2(Ry)$ is the electronically excited $O_2(A^1\Sigma_u^-)$ state with an energy of 4.47 eV; $O_2(v_k)$ ($k = 1, 2, \dots$) are the vibrationally excited states; $O_2(Rot)$ is the first rotational level of an O_2 molecule; and $\Delta\epsilon$ is the electron energy loss in the output channel ($\Delta\epsilon < 0$ for impacts of the second kind). The cross sections for reactions 12, 17, 19, and 33 (impacts of the second kind) are calculated from the cross sections of corresponding direct processes using the detailed balance relation. The rate constants shown in Arrhenius form are taken from [6].

1. A. V. Phelps, JILA Report, No. 28, 1985 ([ftp://jila.colorado.edu/collision data/](ftp://jila.colorado.edu/collision%20data/)).
2. Y. Itikawa and A. Ichimura, Phys. Chem. Ref. Data. **19**, 637 (1990).
3. S. Matejcek, A. Kiender, P. Cicman, *et al.*, Plasma Sources Sci. Technol. **6**, 140 (1997).
4. I. A. Kossyi, A. Y. Kostinsky, A. A. Matveyev, and V. P. Silakov, Plasma Sources Sci. Technol. **1**, 207 (1992).
5. V. V. Ivanov, K. S. Klopovsky, D. V. Lopaev, *et al.*, IEEE Trans. Plasma Sci. **5**, 1279 (1999).
6. www.kinema.com

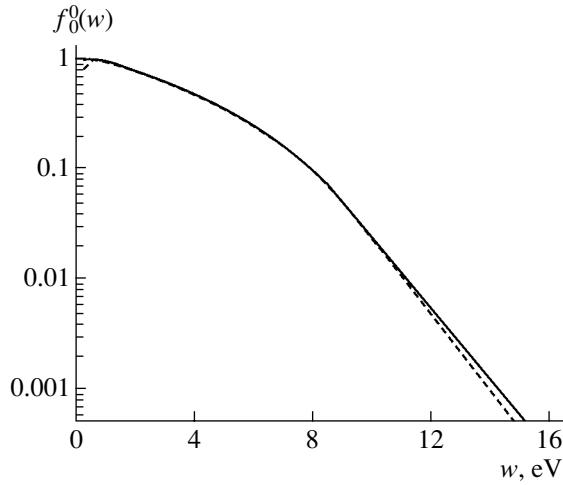


Fig. 1. Local EEDFs for $p = 1$ torr and $i = 50$ mA. The solid curve shows the results of self-consistent calculations for the radius r varying from 0 to R with a step of $R/5$. The dashed curve shows the local EEDF $f_0^0(w)$.

that all the EEDFs are strongly nonequilibrium. For this reason, the rate constants of many plasmachemical processes differ significantly from those obtained in the fluid model, which deals with the temperature T_{ef} (the same for all the electrons). In turn, this leads to a difference in the plasma parameters that significantly depend on these rate constants.

At high pressures, the EEDF is local; i.e., the function $f_0^0(w)$ is independent of r (Fig. 1). At low pressures, the EEDF is not only nonequilibrium but also nonlocal. In this case, the values of $f_0(\epsilon)$ represented as a function of the total energy $\epsilon = w + e\phi(r)$ (i.e., without normalizing and shifting by the space potential) coincide at different radii (Fig. 2a). The same EEDFs $f_0(\epsilon)$ plotted using the conventional local representation as functions of the kinetic energy w (similar to Fig. 1) differ for different radii r (Fig. 2b). In oxygen, the energy loss due to inelastic collisions is dominant over almost the entire energy range. Hence, using the equality $\lambda_\epsilon = \sqrt{\lambda\lambda^*}$ [8] and the total cross sections for elastic and inelastic collisions ($\sigma = 5 \times 10^{-16}$ cm² and $\sigma^* = 5 \times 10^{-17}$ cm², respectively), we obtain the estimate $\lambda_\epsilon \approx 0.2/p$ (in cm), where p is in torr. It follows from the above estimates that, for oxygen, the criterion for the EEDF to be nonlocal ($\lambda_\epsilon > \Lambda$) is $p\Lambda < 0.2$ cm torr, which agrees with the results of our simulations and the data from [12, 18]. Note that, at $\lambda_\epsilon > \Lambda$, the thermal conductivity equalizes the electron temperature over the discharge cross section. This circumstance justifies the use of the space-averaged (global) model [4, 5]. However, due to the unavoidable non-Maxwellian character of the EEDF, the correct application of the space-averaged description is only possible in the frame of the 2T global model [10].

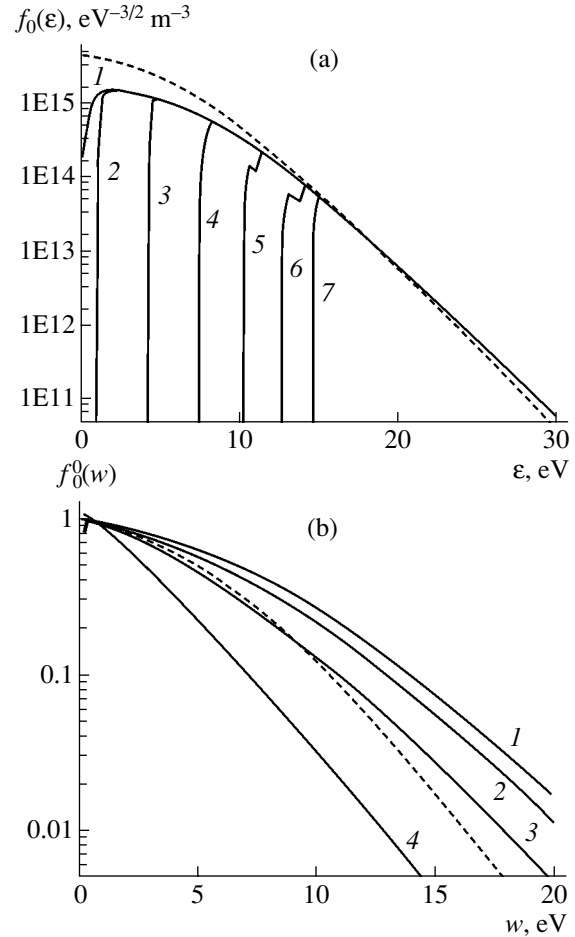


Fig. 2. Nonlocal EEDFs for $p = 0.15$ torr and $i = 50$ mA. (a) The solid curves show the results of self-consistent calculations for the radii $r = (1) 0, (2) 0.6R, (3) 0.8R, (4) 0.69R, (5) 0.95R, (6) 0.98R, (7) R$. The dashed curve shows the local EEDF $f_0^0(w)$. (b) The solid curves show the results of self-consistent calculations for the radii $r = (1) 0, (2) 0.6R, (3) 0.8R, (4) R$. The dashed curve shows the local EEDF $f_0^0(w)$.

For rapid self-consistent estimates of the plasma parameters, it is desirable to have a procedure that takes into account the nonequilibrium and nonlocal character of the EEDF and is less time-consuming than the full-scale (4D) solution of the Boltzmann equation. To date, the most developed and widespread method is the solution of the local kinetic equation with known initial parameters, i.e., with a given reduced field E/N , degree of ionization n_e/N , and degree of excitation n^*/N . This approach can be implemented using available commercial software (e.g., the 0D Boltzmann Solver CFDRC [16, 17], BOLSIG [19], etc.). For comparison, the dashed curves in Figs. 1 and 2 show the EEDF $f_0^0(w)$ determined by solving the local Boltzmann equation (using the 0D Boltzmann Solver [16, 17]) with the same input parameters as in self-consistent calcula-

tions. As was expected, this EEDF is almost the same as that obtained for the pressure $p = 1$ torr (Fig. 1) but significantly differs from that obtained at a lower pressure (Fig. 2b). This means that, in the local regime ($\Lambda > \lambda_e$), one can use any version of the hybrid model with an EEDF determined by solving the local kinetic equation [19]. In particular, Lookup Tables [16, 17] can be used in such a situation. At lower pressures, when the EEDF forms in the nonlocal regime, the EEDFs represented as a function of the kinetic energy are different at different radii and the corresponding local calculation of the EEDF is no longer justified (Fig. 2b). This is also confirmed by the results of directly comparing the local and nonlocal approaches when modeling the positive column of a dc discharge in noble gases (see, e.g., [20]). Under nonlocal conditions of EEDF formation, direct attempts to modernize the fluid model (see, e.g., [21]) seem to be unpromising.

In our opinion, the approach of [10] is more attractive. It was shown in that paper that, for a given value of the parameter $p\Lambda$, the fast part of the EEDF does not depend on the EEDF formation regime (local or nonlocal). Indeed, if we match the fast parts of the EEDFs calculated in the local ($f_0^0(w)$) and nonlocal ($f_0(\epsilon)$) models (e.g., by joining them at an energy close to the ionization threshold), then the tails of both EEDFs will coincide (Fig. 2a). This, at first sight paradoxical result reflects the nature of the discharge as a self-organizing system: to enable its steady-state operation, electron reproduction with a rate depending on the electron loss rate is required. Note that the latter rate is slightly sensitive to the shape of the EEDF.

The aforesaid explains the fact that a real EEDF in a gas-discharge plasma can be, as a rule, satisfactorily approximated by two (or three) electron groups. In [10], the more common approximation by the two exponents was used:

$$f_0(\epsilon) = c_n e^{-\frac{\epsilon}{T_{eb}}} - c_n e^{-\frac{\epsilon_1}{T_{eb}}} (1 - T_{et}/T_{eb}), \quad \epsilon \leq \epsilon_1,$$

$$f_0(\epsilon) = c_n \frac{T_{eb} e^{\frac{\epsilon_1}{T_{et}} - \frac{\epsilon_1}{T_{eb}}}}{T_{eb}} e^{-\frac{\epsilon}{T_{et}}}, \quad \epsilon \geq \epsilon_1, \quad (1)$$

$$c_n \approx 2n_e / \sqrt{\pi T_{eb}^3}.$$

Here, T_{eb} is the temperature of slow (bulk) electrons with $\epsilon < \epsilon_1$ and T_{et} is the temperature of fast (tail) electrons with $\epsilon > \epsilon_1$. In writing approximation (1), it was taken into account that, to ensure the continuity of the energy flux, one should join both the EEDFs themselves and their derivatives at the threshold energy ϵ_1 . For an oxygen plasma, the energy $\epsilon_1 \approx 10$ eV corresponds to the energy threshold for the most efficient processes of dissociative excitation of the high-lying electronic states of an oxygen molecule [22] and is

close to the ionization energy $\epsilon_i = 12$ eV (Figs. 1, 2). Since the behavior of the EEDF tail is close to exponential (see, e.g., Figs. 1, 2), the temperature T_{et} is defined as

$$T_{et} = -(d \ln f_0(\epsilon) / d\epsilon)^{-1}. \quad (2)$$

As a rule, when the electron–electron collision frequency is low, the energy dependence of the distribution function of the bulk electrons ($\epsilon < \epsilon_1$) is nonexponential (Figs. 1, 2). This is related to the fact that the energy balance in low- and moderate-pressure gas discharges is usually determined by inelastic processes with high energy thresholds ($\sim \epsilon_1$). At $w \leq \epsilon_1$, the energy dependence of the EEDF is determined by the behavior of the cross section $\sigma(w)$ for elastic collisions [8]

$$f_0(w) \sim \int_w^{\epsilon_1} (\sigma(w)/w) dw + f_0(\epsilon_1). \quad (3)$$

It seems that such EEDFs are more suitable to approximate by power-law (rather than exponential) functions of energy. These EEDFs depend slightly on the electric field (mainly via the matching constant $f_0(\epsilon_1)$). Since the electrons with energies $\epsilon \leq \epsilon_1$ insignificantly contribute to the total energy balance of the electron gas, their mean energy also slightly depends on the electric field. These electrons acquire the energy from the field in the energy range $(0, \epsilon_1)$ and provide the required electron energy flux toward the EEDF tail [8]. In other words, the low-energy part of the EEDF ($\epsilon < \epsilon_1$) acts as a kind of pipeline from a source at low energies to a sink in the EEDF tail ($\epsilon > \epsilon_1$). The electron density profile along this pipeline does not depend on the energy flux and is only determined by the condition that the energy acquired by low-energy electrons is almost entirely transferred to high-energy electrons. In such a situation, attempts to find the electron temperature from the energy balance equation (see, e.g. [23–25]) seem to be unpromising. However, approximation (1) requires knowledge of the temperature T_{eb} of the slow electrons. The problem can be somewhat simplified because the temperature T_{eb} is only needed to find the characteristics that are slightly sensitive to its value (the plasma ambipolar field; the rate constants of reactions with low energy thresholds, $\epsilon_j \leq T_{eb}$; etc.). Taking this fact into account and assuming that $\sigma(w)$ in formula (3) grows monotonically, we can propose the following approximation for the EEDF (2T EEDF):

$$f_0(\epsilon) = c_n \left(1 - \frac{\epsilon}{\epsilon_1 + T_{et}} \right), \quad \epsilon \leq \epsilon_1,$$

$$f_0(\epsilon) = c_n \frac{T_{et}}{(\epsilon_1 + T_{et})} e^{-\frac{(\epsilon - \epsilon_1)}{T_{et}}}, \quad \epsilon \geq \epsilon_1, \quad (4)$$

$$c_n \approx 15n_e/(4\epsilon_1^{3/2}),$$

which also ensures the conservation of the energy flux at $\epsilon = \epsilon_1$ and depends explicitly only on the temperature T_{et} of the fast electrons. The temperature of the low-energy part ($\epsilon \leq \epsilon_1$) of the EEDF (4) is

$$T_{eb} = 2\bar{\epsilon}_{eb}/3 \approx 0.3(\epsilon_1 + T_{et}).$$

Table 2 presents the characteristic effective temperatures T_j for typical conditions under study, namely, the local regime at $p = 1$ torr and the nonlocal regime at $p = 0.15$ torr. The temperature T_{ef} was found using the fluid model, whereas the temperatures T_{et} , T_{eb} , and T_e were obtained using the kinetic model with allowance for Eq. (2) and formulas

$$T_{eb} = 2 \int_0^{\epsilon_1} f_0(w) w^{3/2} dw / \left(3 \int_0^{\epsilon_1} f_0(w) w^{1/2} dw \right), \quad (5a)$$

$$T_e = 2 \int_0^{\infty} f_0(w) w^{3/2} dw / \left(3 \int_0^{\infty} f_0(w) w^{1/2} dw \right). \quad (5b)$$

As was expected, the temperatures T_e and T_{eb} turned out to be close to each other ($T_e \approx T_{eb}$). At first glance, the temperature T_{ef} , which is found in the fluid model from the energy balance for the entire electron gas, should also be close to T_e and T_{eb} , because it seems that the energy balance for all the electrons would yield the energy of the ‘‘average’’ electron. It happens, however, that the temperature obtained by fluid simulations is significantly lower than the average EEDF temperature ($T_{ef} < T_e$) and is close to the temperature of the EEDF tail ($T_{ef} \approx T_{et}$). On one hand, this fact indicates that the fluid description of electrons is inapplicable to the simulations of a weakly ionized gas-discharge plasma. On the other hand, it explains why the use of the conventional fluid model proved to be surprisingly successful in calculating the main plasma parameters. For electropositive plasma, this is explained by the fact that both the energy loss due to inelastic collisions with high energy thresholds and the ionization processes are determined by the EEDF tail [10]. Hence, roughly speaking, the energy balance and the particle balance are determined by the same temperature T_{et} . Indeed, for a simple plasma, it follows from the condition of steady-state discharge operation that the ionization rate and the loss rate associated with diffusion toward the wall are equal to each other (Schottky condition):

$$v_i \tau_{dp} = 1. \quad (6)$$

This condition determines the eigenvalue $v_i(T_{et})$ of the boundary-value problem for the density of charged particles with $n_e = n_p$. The characteristic time τ_{dp} is determined by the discharge geometry and depends slightly on the EEDF shape. It can be estimated by the

Table 2. Characteristic temperatures in the positive column of a dc oxygen discharge

No.	Regime	T_{ef} , eV	T_e , eV	T_{eb} , eV	T_{et} , eV	T_j , eV
1	150 mtorr–5mA	3.2	3.9	3.1	2.9	2.7
2	150 mtorr–50 mA	2.9	4.1	3.4	2.8	2.7
3	150 mtorr–500 mA	2.9	3.9	3.1	2.9	2.7
4	1 torr–5 mA	1.7	2.6	2.6	1.3	1.5
5	1 torr–50 mA	1.7	2.6	2.6	1.3	1.5
6	1 torr–200 mA	1.7	2.6	2.6	1.4	1.5

interpolation formula (see, e.g., [14])

$$\tau_{dp} = \tau_{ap} + \tau_{bp}. \quad (7)$$

Here, $\tau_{ap} = \Lambda^2/D_{ap}$ is the characteristic time of ambipolar diffusion ($D_{ap} = D_p T_{eb}/T$) and $\tau_{bp} = a\Lambda/V_b$ is the Bohm time, where $V_b = \sqrt{T_{eb}/M}$ and a is a numerical factor on the order of unity. As is seen from Eq. (7), the characteristic time τ_{dp} is determined by the discharge geometry and depends slightly on the EEDF shape. Nevertheless, the ionization frequency depends strongly on the temperature. For example, for a Maxwellian EEDF and the commonly used approximation for the energy dependence of the ionization cross section, $\sigma_i(\epsilon) = \sigma_{0i}(\epsilon/\epsilon_i - 1)$, with the threshold $\epsilon_i \gg T_{et}$, the ionization frequency can be represented in Arrhenius form:

$$v_i = N \int_{\epsilon_i}^{\infty} \sigma_i(w) \sqrt{\frac{2w}{m}} f_0(w) \sqrt{w} dw \approx N \sigma_{0i} \sqrt{\frac{8T_e}{\pi m}} e^{-\frac{\epsilon_i}{T_e}}. \quad (8)$$

For an oxygen plasma with a Maxwellian EEDF, we propose the following approximation for the ionization rate constant:

$$\begin{aligned} k_i &\approx 4 \times 10^{-15} \sqrt{T_e} \exp(-12.06/T_e) \\ &\approx 3 \times 10^{-15} T_e \exp(-12.06/T_e) \text{ m}^3/\text{s}. \end{aligned} \quad (8a), (8b)$$

Condition (6) allows one to reliably calculate the ionization frequency v_i , which is equal to the diffusion loss rate $1/\tau_{dp}$. Since this rate depends slightly (logarithmically) on T_{eb} , it follows from Eqs. (6)–(8) that, for a given gas species, the temperature T_{et} depends only on the parameter $p\Lambda$ [10]. It should be stressed that any EEDF (not necessarily a Maxwellian or Druyvesteyn one) that sharply (exponentially) depends on energy gives more or less close values of the effective temperature of the high-energy part of the EEDF (note that this temperature depends logarithmically on the discharge parameters). On the other hand, if inelastic losses with a high energy threshold ϵ_1 (comparable with the ionization energy ϵ_i) are dominant in the energy balance of the entire electron gas, then we have $T_{ef} \approx T_{et}$. In gas dis-

charges, inelastic energy losses usually exceed elastic ones. Hence, the surprising fact that fluid simulations, as a rule, quite fairly describe the main plasma parameters can be explained by the insensitivity of the calculated results (some kind of “self-healing”) to the shape of the high-energy part of the EEDF. At the same time, the errors in determining the plasma characteristics that are governed by the low-energy part of the EEDF with the temperature T_{eb} (which is different from T_{et}) can be rather large.

To generalize the data of [10] on electronegative gases, we will use scaling laws [14] based on the classification of the regimes of charged particle transport in a discharge.

The main channel for the production of negative ions is dissociative attachment. In the low-pressure range under study ($p\Lambda \leq 1$ cm torr), the processes involving three-body collisions are of minor importance. Hence, the main negative ions are O^- ions, whereas the densities of O_2^- and O_3^- ions are low and do not affect the balance of charged particles. The main ionization mechanism is the direct ionization of O_2 molecules; consequently, the main positive ions are O_2^+ ions, whereas the density of O^+ ions is significantly lower.

At $p\Lambda < 1$ cm torr and the degrees of ionization considered in this study ($n_e/N < 10^{-4}$), the recombination loss rate of positive ions is smaller than the loss rate associated with diffusion toward the wall (the latter can be again estimated using Eq. (7)).

It is known (see, e.g., [9]) that the plasma of electronegative gases is characterized by the presence of an outer electron-ion plasma shell (“skin”), in which negative ions are practically absent. Although the skin is usually very thin, its presence is of principal importance because it confines the negative ions inside the volume. Discharges in electronegative gases are characterized by an extra degree of freedom, namely, the degree of electroneutrality. In a simple model that describes the processes of attachment, detachment, ionization, and recombination with the help of phenomenological coefficients K_a , K_d , K_i , and K_r [9, 14], the parameters of an electronegative-gas plasma depend on the relation between the attachment time $1/v_a$ and diffusion time τ_{an} (which is determined by the electron temperature T_{eb}) of the negative ions, i.e., on the parameter $v_a\tau_{an}$. The dependences obtained in [9, 14] allow one to find the temperature T_{et} using the following simple considerations. Since the flux of negative ions toward the wall is zero, from the balance of negative and positive ions, we obtain the following relationships for the densities \bar{n} averaged over the discharge cross section:

$$v_a\bar{n}_e = v_a\bar{n}_n + K_r\bar{n}_n\bar{n}_p, \quad (9)$$

$$v_i\bar{n}_e = \bar{n}_p/\tau_{dp}, \quad (10)$$

where v_a is the attachment frequency, v_d is the detachment frequency, and K_r is the rate constant for ion-ion recombination. The positive ion density n_p is equal to the sum of the negative ion density n_n and the electron density n_e : $n_p = n_n + n_e$.

At low pressures ($\tau_{an}v_a < 1$), the negative ions obey a Boltzmann distribution and their density profile is parabolic, whereas the electron density profile is flat. In this regime, the ionization rate exceeds the attachment rate [9, 14] and, at the discharge periphery (in the electron-ion skin), the equality $n_e = n_p$ is satisfied. At low pressures, the skin thickness is smaller than the particle mean free path; hence, using Eqs. (7) and (10), we obtain the simple expression

$$v_i\tau_{bp} = 1, \quad (11)$$

which can be used to find the temperature T_{et} .

Using approximation (8a) for the ionization rate constant in oxygen, we obtain the analytic expression for T_{et} :

$$T_t = \varepsilon_1/(\ln 2286p\Lambda), \quad (12)$$

which depends only on the parameter $p\Lambda$ (here, the pressure p is in torr and Λ is in cm).

Expression (11), which is similar to Eq. (6) for an ordinary plasma, can be used to find the temperature T_e in an electronegative plasma (see [1]). This expression has been widely used when analyzing the plasmas of electronegative gases (see, e.g., [2, 3–5, 13, 15]). However, we note that expression (11) is only applicable when $v_a\tau_{an} < 1$, which, in the case of oxygen, corresponds to the condition $p\Lambda < 0.1$ cm torr. In [26], it was shown that the approach of [1], which is based on the assumption that not only the electrons but also the ions obey a Boltzmann distribution, cannot be extended to the higher pressure range.

At elevated pressures ($p\Lambda > 0.1$ cm torr), the condition $v_a\tau_{an} > 1$ is satisfied and the ionization rate is less than the attachment rate [9, 14]. In this case, the situation substantially depends on the volume loss of negative ions. In oxygen, the inequality $\tau_{an}v_a > 1$ means the occurrence of the detachment regime; i.e., the loss of negative ions is governed by detachment (rather than recombination). In this case, various types of flat-top profiles of the electron and ion densities can be established (see [9, 14, 26] for details). Hence, from Eqs. (9) and (10) we have

$$v_i\tau_{ap}/(1 + \bar{n}_n/\bar{n}_e) = v_i\tau_{ap}/(1 + v_a/v_d) = 1, \quad (13)$$

which, with allowance for Eq. (8a), gives a simple analytic estimate for the temperature T_{et} :

$$T_t = \varepsilon_1/[2\ln(182p\Lambda) - \ln(1 + v_a/v_d)] \approx \varepsilon_1/(2\ln(182p\Lambda)), \quad (14)$$

where pressure p is in torr and Λ is in cm.

The results of calculating T_t by formulas (12) and (14) are also presented in Table 2. These simple expressions are seen to agree well with both the EEDF tail temperature T_{et} obtained by the kinetic model and the average electron temperature T_{ef} obtained by fluid simulations.

From the kinetic equation for the temperature of the high-energy part of the EEDF, we have the simple estimate

$$T_{et} = \sqrt{\sum_j \nu_j / D_E}, \quad (15)$$

where $D_E = 2(eE\lambda)^2 v / 3$ is the energy diffusion coefficient in an electric field (see, e.g., [8] for details). Since it is the electric field that delivers energy to electrons, the temperature T_{et} and, consequently, the ionization frequency ν_i are governed by the heating electric field, which is either the longitudinal field (in the positive column under study) or the averaged high-frequency field $\langle E_{eff} \rangle$ (in rf and microwave discharges). For this reason, when analyzing the EEDF (see, e.g., [27]) or developing user's software for computing the EEDF (see, e.g., [19]), the electric field is usually assumed to be given. However, in any problem of plasma physics, neither fields nor particle motion can be treated as given, because the fields are specified not only by the external conditions, but also by the charged particle motion, which, in turn, is governed by the fields. Hence, all the problems are self-consistent: the plasma allows only those fields in the discharge volume that are required for this plasma to exist. The ionization rate is specified by the EEDF shape (the T_{et} temperature), which is determined by the fields in the plasma. On the other hand, it is necessary that the production of the charged particles balances their losses, which depend mainly on the discharge geometry and the pressure ($p\Lambda$). As a result, the heating field, which can be obtained from expression (15) using the temperature T_{et} deduced from Eqs. (6)–(14), is also governed by the parameter $p\Lambda$ [10]. We note in this context that the spatial distribution of the self-consistent fields in the plasma volume is not known *a priori* and, in contrast to the case of the positive column of a dc discharge, which has been considered in this study, the problem of determining the field profiles in the plasmas of various discharges (ECR, ICP, SW, etc.) is a difficult problem by itself. In such discharges, attempts to find T_{et} as a function of the average effective heating field $\langle E_{eff} \rangle$ via relations similar to expression (15) are very laborious and lead to rather sophisticated expressions that are difficult to handle (see, e.g., [28]).

Let us now consider the reasons why the mean electron energy $\bar{\epsilon}_{ef} = 3T_{ef}/2$, which was obtained in fluid simulations from the energy balance equation for all the electrons, turned out to be close to the temperature T_{et} of the high-energy part of the EEDF, rather than to the

mean energy of the electron gas $\bar{\epsilon}_e = 3T_e/2$. An analysis of the energy balance equation for all the electrons shows that, for an oxygen dc discharge, the most efficient channels of energy losses are the reactions of dissociative excitation of the high-lying electronic states of an oxygen molecule with energy thresholds of 7–10 eV ($\epsilon_1 \approx 10$ eV) and ionization ($\epsilon_i = 12$ eV). Since the efficiency of these processes is determined by the high-energy part of the EEDF, then, for a Maxwellian EEDF, we have $T_{ef} \approx T_{et}$. We note that, for steady-state low-pressure discharges, both the electron energy balance and ionization are almost always (especially in atomic gases) determined by the processes with high thresholds. Hence, the results obtained in this study apply to all these cases. If the energy balance is determined by elastic processes or inelastic processes with low thresholds (quasi-elastic processes), then the situation changes insignificantly. In this case, only the shape of the low-energy part of the EEDF changes, whereas the high-energy part of the EEDF and its temperature T_{et} are again governed by the balance between ionization and diffusion losses (see Eqs. (6)–(14)). The energy balance equation, as well as calculations by the fluid model, give the temperature T_{eb} of the low-energy part of the EEDF, and the dc (or rf) discharge current is expressed in terms of the specific power W deposited in the discharge (or the longitudinal electric field in the case of a dc discharge). Such a situation occurs, in particular, in gases in which the energy loss due to vibrational excitation is dominant (e.g., in nitrogen, carbon oxide, etc.), provided that the gas pressure is not too low. Particular features of such discharges can easily be taken into account by applying the 2T fluid model proposed here.

The increase in the degree of ionization caused by an increase in the discharge current (an increase in the specific power W deposited in the discharge) leads to the Maxwellianization of the EEDF due to electron–electron collisions. According to Eqs. (6)–(14), with given external conditions and given ionization and loss mechanisms, the temperature T_{et} of the high-energy part of the EEDF remains almost unchanged. Therefore, as the electron–electron collision frequency increases, the temperature T_{et} of the low-energy part of the EEDF changes and approaches the constant temperature T_{et} of the EEDF tail. This process is accompanied by a decrease in D_E (and, consequently, in the electric field). In other words, the paradigm of the problem changes radically because, in the literature, the change of the EEDF with increasing electron density at a constant electric field is usually considered; in this case, both the body and the tail of the distribution function vary with increasing degree of ionization. However, according to [10] and the above analysis, in a steady-state discharge occupying a fixed volume, the temperature T_{et} of the high-energy part of the EEDF remains nearly constant. For this reason, the increase in the electron–electron collision frequency with increasing deposited power

(current) leads to a change of only the low-energy part of the EEDF; i.e., the temperature T_{eb} of the low-energy part of the EEDF approaches the constant temperature T_{et} of the EEDF tail.

In all the discharges, as the degree of ionization and the electron–electron collision frequency increase further ($n_e T_e v_e \gg W$), the EEDF becomes Maxwellian with a single temperature that coincides with the temperature of fast electrons and depends only on $p\Lambda$.

Thus, using commercial CFDRC software (<http://www.cfdrc.com/~cfdplasma>), we compared the kinetic and fluid approaches to modeling the plasma of the positive column of a dc oxygen discharge. It is shown that for both local and nonlocal regimes of EEDF formation, the non-Maxwellian EEDF can be adequately approximated by two groups of electrons. The condition of steady-state discharge operation allows one to determine the temperature T_{et} of the fast electrons as an eigenvalue of the problem. For a given gas species, this temperature is a function of the parameter $p\Lambda$ and weakly (logarithmically) depends on the external conditions. The energy balance for the entire electron gas does not allow one to find the characteristic temperatures that are of practical interest. To calculate the parameters of a gas-discharge plasma, we propose the 2T fluid model, which allows one to incorporate the main characteristics of a nonequilibrium and nonlocal EEDF into the conventional fluid model.

ACKNOWLEDGMENTS

One of the authors (L.D. Tsendin) acknowledges the support of the Russian Foundation for Basic Research (project no. 01-02-16874) and NATO SFP (grant no. 974354).

REFERENCES

1. M. Lieberman and A. Lichtenberg, *Principles of Plasma Discharges and Materials Processing* (Wiley, New York, 1994).
2. I. G. Kouznetsov, A. J. Lichtenberg, and M. A. Lieberman, *Plasma Sources Sci. Technol.* **5**, 662 (1996).
3. J. D. Bukowski, D. B. Graves, and P. J. Vitello, *Appl. Phys.* **80**, 2614 (1996).
4. C. Lee and M. A. Lieberman, *J. Vac. Sci. Technol. A* **13**, 368 (1995).

5. J. T. Gudmindsson, I. G. Kouznetsov, K. K. Patel, *et al.*, *J. Phys. D* **34**, 1100 (2002).
6. I. P. Shkarofsky, T. W. Johnson, and M. P. Bachynski, *The Particle Kinetics of Plasmas* (Addison–Wesley, Reading, 1966).
7. A. A. Kudryavtsev and L. D. Tsendin, *Zh. Tekh. Fiz.* **69** (11), 34 (1999) [*Tech. Phys.* **44**, 1290 (1999)].
8. L. D. Tsendin, *Plasma Sources Sci. Technol.* **4**, 200 (1995).
9. A. V. Rozhansky and L. D. Tsendin, *Transport Phenomena in Partially Ionized Plasma* (Taylor & Francis, London, 2001).
10. A. A. Kudryavtsev and L. D. Tsendin, *Pis'ma Zh. Tekh. Fiz.* **28** (20), 7 (2002) [*Tech. Phys. Lett.* **28**, 841 (2002)].
11. G. Gousset, C. M. Ferreira, M. Pinheiro, *et al.*, *J. Phys. D* **24**, 290 (1991).
12. V. V. Ivanov, K. S. Klopovsky, D. V. Lopaev, *et al.*, *IEEE Trans. Plasma Sci.* **27**, 1279 (1999).
13. J. T. Gudmindsson, A. M. Marakhtanov, K. K. Patel, *et al.*, *J. Phys. D* **33**, 1323 (2000).
14. E. A. Bogdanov, V. I. Kolobov, A. A. Kudryavtsev, *et al.*, *Zh. Tekh. Fiz.* **72** (8), 13 (2002) [*Tech. Phys.* **47**, 946 (2002)].
15. M. W. Kiehbauch and D. B. Graves, *J. Appl. Phys.* **91**, 3539 (2002).
16. *CFD–PLASMA: User's Manual* (CFD, Huntsville, 1999–2002).
17. <http://www.cfdrc.com/~cfdplasma>.
18. V. V. Ivanov, K. S. Klopovsky, D. V. Lopaev, *et al.*, *J. Plasma Phys.* **26**, 970 (2000).
19. <http://www.siglo-kinema.com/BOLSIG>: Boltzmann Solver for the SIGLO-series.
20. J. Behnke, Yu. Golobovsky, S. U. Nisimov, *et al.*, *Contrib. Plasma Phys.* **36** (1), 75 (1996).
21. J. H. Ingold, *Phys. Rev. E* **56**, 5932 (1997).
22. B. Eliassen and V. Kogelsschalz, *J. Phys. B* **19**, 1241 (1986).
23. W. L. Morgan and L. Vriens, *J. Appl. Phys.* **51**, 5300 (1980).
24. J. T. Dakin, *J. Appl. Phys.* **60**, 563 (1986).
25. A. Harters and J. A. M. van der Mullen, *J. Phys. D* **34**, 1907 (2001).
26. R. N. Franklin and J. Snell, *J. Phys. D* **32**, 2190 (1999).
27. V. L. Ginzburg and V. L. Gurevich, *Usp. Fiz. Nauk* **70**, 201 (1960) [*Sov. Phys. Usp.* **70**, 115 (1960)].
28. T. Kimura and K. Oke, *J. Appl. Phys.* **89**, 4240 (2001).

Translated by N. Ustinovskii